Fermilab

TM-1108
1183.000

CHARACTERISTICS OF A-150 PLASTIC-EQUIVALENT GAS in A-150 PLASTIC IONIZATION CHAMBERS FOR p(66)Be(49) NEUTRONS.

July 8, 1982

M. Awschalom
I. Rosenberg
R. K. Ten Haken

Neutron Therapy Facility
Fermilab, P. O. Box 500
Batavia, Illinois 60510

D. W. Pearson
F. H. Attix
P. M. DeLuca

Department of Medical Physics
University of Wisconsin
Madison, Wisconsin 53706

ABSTRACT

The evaluation of a gas mixture having an atomic composition similar to that of A-150 TE-plastic has been extended to a high energy neutron therapy beam. "A-150" gas, air and methane-based TE gas were each flowed through A-150 plastic-walled ion chambers of different sizes and irradiated with p(66)Be(49) neutrons. A tentative value for $\overline{W}$(A-150) of 27.3 $\pm$0.5 J C^{-1} was derived for this beam. The $\overline{W}$ value of the A-150 gas mixture is compared to those of methane-based TE gas and of air for the p(66)Be(49) neutron beam as well as to corresponding values found in similar experiments using 14.8 MeV monoenergetic neutrons.

KEY WORDS: gas mixture, ion chamber, TE gas, $\overline{W}$, neutrons, dosimetry.

Introduction

The use of an ionization chamber filled with a gas having the same atomic composition as its walls would simplify the application of Bragg-Gray cavity theory and eliminate the cavity-size dependence of W, the mean energy needed to form an electron-ion pair.[1] Various gas mixtures that closely approximate the atomic composition of A-150 plastic[2] have been proposed by Awschalom and Attix[3]. Initial measurements of the properties of one of these mixtures have been made in ^{60}Co and 14.8 MeV neutron radiation fields.[4] This paper presents measurements made in the p(66)Be(49) neutron therapy beam at the Fermilab Neutron Therapy Facility.[5] Detailed discussions of the rationale and theoretical considerations for these measurements have been given elsewhere.[4] Briefly, several different size chambers with A-150 plastic walls were irradiated in the neutron beam while filled with one of three different gas mixtures: air, methane-based TE gas[6] or the selected A-150 gas.[3] Then, if Bragg-Gray cavity conditions are satisfied (see appendix to Ref. 4), the ratio of the normalized charges created by ionization of any two gases in each chamber can be related to the ratio of the $\overline{W}$ values for those two gases. Using the accepted values of $\overline{W}$ for air and tissue equivalent gas, the value of $\overline{W}$ for A-150 gas may then be obtained.

Experimental Arrangements

Many of the experimental details of this investigation were very similar to those described in a preceding paper.[4]

1. Gases and Gas Handling.

The same mixtures used in the previous investigation[4] were also used here. Some of their properties are summarized in Table 1. The same gas handling was also used.

2. Ionization chambers.

The five ionization chambers used in the present measurements were the same ones used in the previous experiment.[4] Snugly fitting spherical shells brought the total wall thickness of all spherical chambers to 1.12 g cm^{-2}, almost sufficient to reach the depth of maximum dose.[7] All chambers and buildup caps are made out of A-150 TE-plastic. They are:

a)

Parallel plate chamber. Designed and constructed by J. J. Spokas of Illinois Benedictine College in consultation with Fermilab. It has a circular collector of 1 cm radius, plate separation of 1 mm, total volume of 0.3 cm^3, and a 0.5 mm entrance window. It is embedded in a large A-150 disk. Additional A-150 disks provided a total build-up thickness of 1.49 g cm^{-2} in front of the chamber and 13 g cm^{-2} behind it.

b)

1 cm^3 spherical ionization chamber, Model IC-17, Serial No. 356 RTG (Far West Technology, Goleta, CA. 93017).

c)

1 cm^3 spherical ionization chamber, Model IC-17, Serial No. 193 TG (EG&G Inc., Goleta, CA. 93017).

d)

8 cm^3 spherical ionization chamber. Designed and constructed at the University of Wisconsin.

e)

80 cm^3 spherical ionization chamber, EG&G Model IC-80, Serial No. 396-8TG.

3. Irradiation Conditions.

The p(66)Be(49) neutron therapy beam at the Fermilab Neutron Therapy Facility was collimated[8] to obtain a 36 cm diameter field size at the positions of the chambers. Figure 1 shows the experimental layout. Two different source-to-detector distances were used on separate occasions. The parallel plate chamber, one 1 cm^3 chamber (#356 RTG) and the 8 cm^3 chamber were irradiated 190 cm from the target. The 80 cm^3

chamber and the other 1 cm^3 chamber (#193 TG) were irradiated at about 350 cm from the target.

4. Measurement Sequences.

Two different sets of measuring electronics were used, a Keithley 602 electrometer[9] or a microcomputer based system described elsewhere.[10,11] Using either system, measurements were reproducible with a precision between $\pm$0.5% and $\pm$1.0%.

Each chamber was cycled through the three available gases, always starting and ending with air. For each set of gas measurements, the chamber high voltage was cycled through a standard sequence, spanning $\pm$300 V to $\pm$1000 V, starting and ending at +600 V.

Results and Discussion

In each instance the collected charge was normalized to the corresponding readings of the dual monitoring transmission ionization chambers. Measurements differed only slightly with change in polarizing voltage sign and they were averaged before analysis.

1. Efficiency of Charge Collection.

The linear accelerator at Fermilab operates in a pulsed mode, delivering 66 MeV protons onto a Be-target in 45 μsec wide pulses at a rate of 15 Hz. Each pulse produces a neutron dose of approximately 0.3 mGy (1/30 rad) at 190 cm from the target. Thus, the instantaneous dose rate is high, and volume recombination of ions in the gas could be significant. Although the ion mobility and recombination coefficients for the gases under study are not well known, except for air,[12] it was assumed that the drift times of the ions were such that the formalism for pulsed beam saturation could apply.[12] Using this formalism in the near-saturation approximation, a linear relationship may be derived between 1/q and 1/V, where q is the collected charge for an applied potential V.

Because of the presence of high LET particles, such as alphas and carbon and oxygen recoils, initial recombination losses must also be considered.[13] The precise formalism involves the Jaffé function f($\underline{x}$), where $\underline{x}$ is a dimensionless parameter proportional to V^2. For sufficiently large values of $\underline{x}$, f($\underline{x}$) becomes proportional to 1/V, and a linear relationship between 1/q and 1/V is again predicted.[12] Using the constants derived for ionization of CO_2 and air by polonium α-particles,[12] and assuming tracks are formed at random angles to the electric field, it is estimated that the relationship is valid even for the 80 cm^3 chamber at 300 V bias.

Based on the above considerations, the inverse normalized collected charge, 1/q, was plotted versus the inverse polarizing voltage, 1/V, for all chambers. The saturation charge per monitor unit was obtained from the intercept derived by a least squares fit to the data. These curves are shown in Fig. 2 for each chamber size and for all three gases. In this figure, all charges were normalized to the saturation values. It can be seen from Fig. 2 that the A-150 gas has the worst saturation properties and air the best, in agreement with previous results found using a monochromatic 14.8 MeV neutron beam.[4] The different slopes observed for the two 1 cm^3 chambers may reflect the 3 to 1 difference in the dose rates at 190 cm and 350 cm from the target. If this is the case, the charge collection losses are due in part to volume recombination, since initial recombination is independent of dose rate.[12]

2. Influence of chamber size.

The ratio of the saturation-corrected charges per monitor unit for an ionization chamber irradiated under identical conditions with two different gases in its cavity is related to the ratio of the $\overline{W}$s of the two gases. However, for chambers not satisfying the Bragg-Gray conditions this relation is a complicated, and usually unknown, function of the ratios of both the mass stopping powers and the kermas of the two gases, as shown in the appendix to Ref. 4. For very small chambers, which satisfy Bragg-Gray conditions, the relation is of the form:

$$\frac{Q_1}{Q_2} = \frac{(S/\rho)_1}{(S/\rho)_2} \frac{\overline{W}_2}{\overline{W}_1} \frac{\rho_1}{\rho_2} \tag{1}$$

where Q is the normalized saturation charge, (S/ρ) is the mass collision stopping power, ρ is the gas density, $\overline{W}$ is the average energy required to produce an electron-ion pair, and 1, 2 refer to the two gases in question. For very large chambers, however, the stopping power ratios should be replaced by the average kerma ratios for the two gases.[1] As can be seen from Table 1, there exists a much larger variation in kermas than in stopping powers among the three gases. Thus, one would expect a monotonic change in the ionization ratios with chamber dimensions.

By extrapolating ionization ratios to infinitesimal chamber size, Bragg-Gray conditions are satisfied and Equation 1 can then be utilized. The observed ratios of ionization charge for A-150 gas to air, A-150 gas to TE gas and, as a consistency check, for TE gas to air were, therefore, plotted in Fig. 3 as a function of mean chord length ℓ for each chamber. For the parallel plate chamber, the plate separation of 1 mm was taken as this length. For the spherical chambers, ℓ was taken as 2/3 of the cavity diameter, assuming spherical volumes, i.e., 8.3 mm, 16.5 mm and 35.6 mm for the 1 cm^3, 8 cm^3 and 80 cm^3 chambers, respectively. It can be seen from Fig. 3 that trends with chamber size are indeed visible. These trends are consistent with the relative values shown in Table 1.

The values of each ionization ratio appropriate for zero chamber size are shown in Fig. 3. They were obtained by extrapolation of a linear least squares fit to the data. The uncertainties in these extrapolated values, arising from the uncertainties in the individual measurements and in the fitting procedures, are on the order of 1-2%.

3. Calculations of $\overline{W}$ ratios and $\overline{W}$ values.

The extrapolated values for the ionization ratios shown in Fig. 3 were combined with the appropriate data from Table 1, according to Equation 1, to obtain estimates of $\overline{W}$ ratios. These ratios are shown in Table 2 together with corresponding ratios for 14.8 MeV neutrons obtained in a previously reported experiment.[4] The ratios $\overline{W}$(TE)/$\overline{W}$(air) and $\overline{W}$(A-150)/$\overline{W}$(air) are seen to be about 2-3% different for the two neutron beams. The significance of these differences is marginal in view of the 1-2% uncertainties in the ionization ratios and the uncertainty in the values of the stopping powers.

From the $\overline{W}$ ratios above, one can obtain estimates of an effective $\overline{W}$(A-150), if values for $\overline{W}$(air) and $\overline{W}$(TE gas) are assumed to be known. There are, however, no $\overline{W}$ values available for the p(66)Be(49) neutron energy spectrum, or even for 25 MeV monoenergetic neutrons. Therefore, the same reference $\overline{W}$ values were used here as those previously adopted for the 14.8 MeV neutrons,[4] although their appropriatness for the higher energy beam is in doubt. These values are given in the notes to Table 3. The differences in $\overline{W}$(A-150) for the two beams, also shown in Table 3, reflect the differences in $\overline{W}$ ratios noted above. The value of $\overline{W}$(A-150) for the Fermilab beam is, however, less reliable in view of the uncertainties in the $\overline{W}$ values used to derive it.

Conclusion.

Values of the ratios of $\overline{W}$ for A-150 gas to the $\overline{W}$s for air and for methane-based TE gas have been obtained for the p(66)Be(49) neutron beam and compared to earlier results obtained using 14.8 MeV neutrons. Absolute values of $\overline{W}$ for all gases, however, are uncertain for the high energy neutron beam and some further work should be undertaken to obtain $\overline{W}$ values appropriate for this spectrum.

Recommendation.

Comparison of ionometric and calorimetric dosimetry results offers an absolute way of determining the product:

$$\frac{\overline{W}}{e} \frac{(S/\rho)_w}{(S/\rho)_g} = \frac{D_w M_g}{Q} \qquad (2)$$

where $\overline{W}/e$ is given in J C^{-1}, D_w is the absorbed dose (J kg^{-1}) in the calorimeter medium (which may be A-150 plastic), M_g is the mass of gas (kg) in the ion chamber and Q(C) is the charge produced in that gas. In the case of A-150 gas, (S/ρ)wall/(S/ρ)gas is unity and $\overline{W}/e$ is thus directly obtained. Such an experiment is under consideration as the next logical step in studying the properties of A-150 and TE gases for use in fast neutron beam dosimetry.

Acknowledgements.

We are grateful to Mr. William M. Quam, EG&G, Goleta, California, who graciously lent us the 80 cm^3 A-150 TE ionization chamber, and to M. C. Schell of the University of Wisconsin Department of Medical Physics who assisted in processing the data. We also with to thank Ms. Michelle Gleason for accurate and untiring retypings of this manuscript. This investigation was supported by PHS Grant Number 5P01CA18081-07, awarded by the National Cancer Institute, DHHS. University of Wisconsin support was provided by the U.S. Department of Energy under contract No. DE-AC02-76EV01105.

REFERENCES

1. T. E. Burlin in "Radiation Dosimetry", edited by F. H. Attix and W. C. Roesch, (Academic Press, New York: 1966), Vol. I, Chapt. 8.

2. J. B. Smathers, V. A. Otte, A. R. Smith, P. R. Almond, F. H. Attix, J. J. Spokas, W. M. Quam, and L. J. Goodman, Composition of A-150 Tissue Equivalent Plastic, Med. Phys. 4, 74 (1977).

3. M. Awschalom, and F. H. Attix, A-150 Equivalent Gas, Phys. Med. Biol. 25, 567 (1980).

4. P. M. DeLuca, F. H. Attix, D. W. Pearson, and M. Awschalom, Application of A-150 Plastic-Equivalent Gas in A-150 Plastic Ionization Chambers for ^{60}Co γ-Rays and 14.8 MeV Neutrons, Med. Phys., 9, 378 (1982).

5. L. Cohen, and M. Awschalom, The Cancer Therapy Facility at the Fermi National Accelerator Laboratory: A Preliminary Report, Applied Radiol. 5, (#6) 51 (1976).

6. H. H. Rossi in "Radiation Dosimetry", edited by G. J. Hine and G. L. Brownell, (Academic Press, New York: 1956).

7. M. Awschalom and I. Rosenberg, Characterization of a p(66)Be(49) Neutron Therapy Beam. II. Skin-Sparing and Dose Transition Effects, Med. Phys. 8, (#1) 105-107 (1981).

8. I. Rosenberg and M. Awschalom, Characterization of a p(66)Be(49) Neutron Therapy Beam: I. Central Axis Depth Dose and Off-axis Ratios, Med. Phys. 8, (#1) 99-104 (1980).

9. Keithley Instruments Company, Cleveland, Ohio 44139.

10. M. Awschalom and I. Rosenberg, Neutron Beam Calibration and Treatment Planning, Fermilab Internal Report TM-834, Dec. 1978.

11. M. Awschalom, R. Goodwin, L. Grumboski, I. Rosenberg, and M. Shea, High Precision in Dose Delivery: Routine Use of a Microcomputer, in Proceedings of International Symposium on Biomedical

Dosimetry: Physical Aspects, Instrumentation, Calibration, Vienna, Austria, 1981.

12. J. W. Boag in "Radiation Dosimetry", edited by F. H. Attix and W. C. Roesch, (Academic: New York 1966), Vol. II., Chapt. 9.

13. J. W. Boag, Cavity Theory and Its Practical Implications for Neutron Dosimetry with Ionization Chambers, in "Ion Chambers for Neutron Dosimetry", p. 151, Ed. Broerse, J. J., Harwood Academic Publishers: New York, 1980.

14. H. H. Anderson and J. F., Zeigler, "Hydrogen Stopping Powers and Ranges in all Elements", New York: Pergamon Press, 1977.

15. M. Awschalom, I. Rosenberg and A. Mravca, Kermas for Various Substances Averaged Over the Energy Spectra of Fast Neutron Therapy Beams, Submitted for publication.

16. ICRU Report 31, Average Energy Required to Produce an Ion Pair, ICRU Publications, P. O. Box 30165,

Washington, D. C., 10014, 1979.

17. L. J. Goodman and J. J. Coyne, W_n and Neutron Kerma for Methane-Based Tissue-Equivalent Gas, Radiat. Res. 82, 13 (1980).

Table Captions

Table 1. Summary of Various Properties of Gases and A-150 Plastic for p(66)Be(49) Neutrons.

Notes:

(a) For gases, in units of mg cm^{-3}, at STP, calculated assuming ideal gas law. For A-150 plastic, in units of g cm^{-3}.

(b) Mass collision stopping powers from Anderson and Zeigler.[14] In units of MeV cm^2 g^{-1}, evaluated at an approximate mean proton energy (under charged particle equilibrium) of 5 MeV, corresponding to monoenergetic 25 MeV neutrons (close to the mean energy of 27 MeV of the Fermilab beam).

(c) From recent kerma calculations for p(66)Be spectrum.[15] In units of 10^{-15} J kg^{-1} m^2 n^{-1}.

(d) Assumed equal to A-150 plastic value.

(e) Compositions of TE gas: Ref. 6; of A-150 gas: Ref. 3, and of A-150 plastic: Ref. 2.

Table 2. Summary of W Ratios.

Notes:

(a) This work, based on ionization ratios in Figure 3 extrapolated to zero chamber size.

(b) From Ref.4, averaged over all chamber sizes.

Table 3. Summary of $\overline{W}$ Values (in J C^{-1}).

Notes:

1 J C^{-1} = 1 eV/electron-ion pair

(a) Assumed $\overline{W}$ (dry air) = 35.1 J C^{-1} from ICRU 31,[16] for 5 MeV α-particles and 1.8 MeV protons.

(b) Assumed $\overline{W}$(TE) = 31.1 J C^{-1} from Goodman and Coyne[17] for 14 MeV neutrons.

(c) These $\overline{W}$ values are based upon reference values given in notes (a) and (b), which are more relevant to 14 MeV neutrons, for lack of more appropriate $\overline{W}$ data at higher energies.

Table 1

Summary of Various Properties of Gases and

A-150 Plastic for p(66)Be(49) Neutrons.

	Air (Dry)	TE Gas	A-150 Gas	A-150 Plastic
Density [(a)]	1.293	1.149	1.442	1.12
Stopping Power [(b)]	68.2	80.2	81.1	81.2
Kerma Factor [(c)]	2.82	6.38	6.51 [(d)]	6.51
Atomic Composition (% by mass) [(e)]	- - N(75.5), O(23.2) Ar(1.3), -	H(10.2), C(45.6) N(3.5), O(40.7) - -	H(10.2), C(76.8) N(3.6), O(5.9) F(1.7), Ar(1.8)	H(10.2), C(76.3) N(3.6), O(5.9) F(1.7), Ca(1.8)

Table 2

Summary of $\overline{W}$ Ratios

Neutron Beam	$\frac{\overline{W}_{TE}}{\overline{W}_{air}}$	$\frac{\overline{W}_{A-150}}{\overline{W}_{air}}$	$\frac{\overline{W}_{A-150}}{\overline{W}_{TE}}$	Notes
p(66)Be(49)	0.858	0.765	0.823	(a)
d+T (14.8 MeV)	0.896	0.813	0.907	(b)

Table 3

Summary of $\overline{W}$ Values (in J C^{-1})

Neutron Beam	$\overline{W}_{TE}$ (from air)	$\overline{W}_{A-150}$ (from air)	$\overline{W}_{A-150}$ (from TE)	Notes
p(66)Be(49)	30.3	26.9	27.8	(c)
d+T (14.8 MeV)	31.4	28.5	28.2	
Notes	(a)	(a)	(b)	

Figure Captions

Fig. 1. Experimental layout.

The neutron beam was collimated to fully cover all chambers at each irradiation position.

The spherical ion chambers were placed just in front of the parallel plate chamber, without shadowing its collecting volume.

Fig. 2. Correlation between 1/q and 1/V for all chambers in the p(66)Be(49) neutron beam.

All charges Q_x were normalized to the monitor chamber charges Q_m, in such a way that the saturation values are unity.

Fig. 3. Saturation ionization ratios in the p(66)Be(49) neutron beam as a function of mean chord length ℓ of the ionization chambers.

Values of these ratios extrapolated to zero chamber size are also shown.

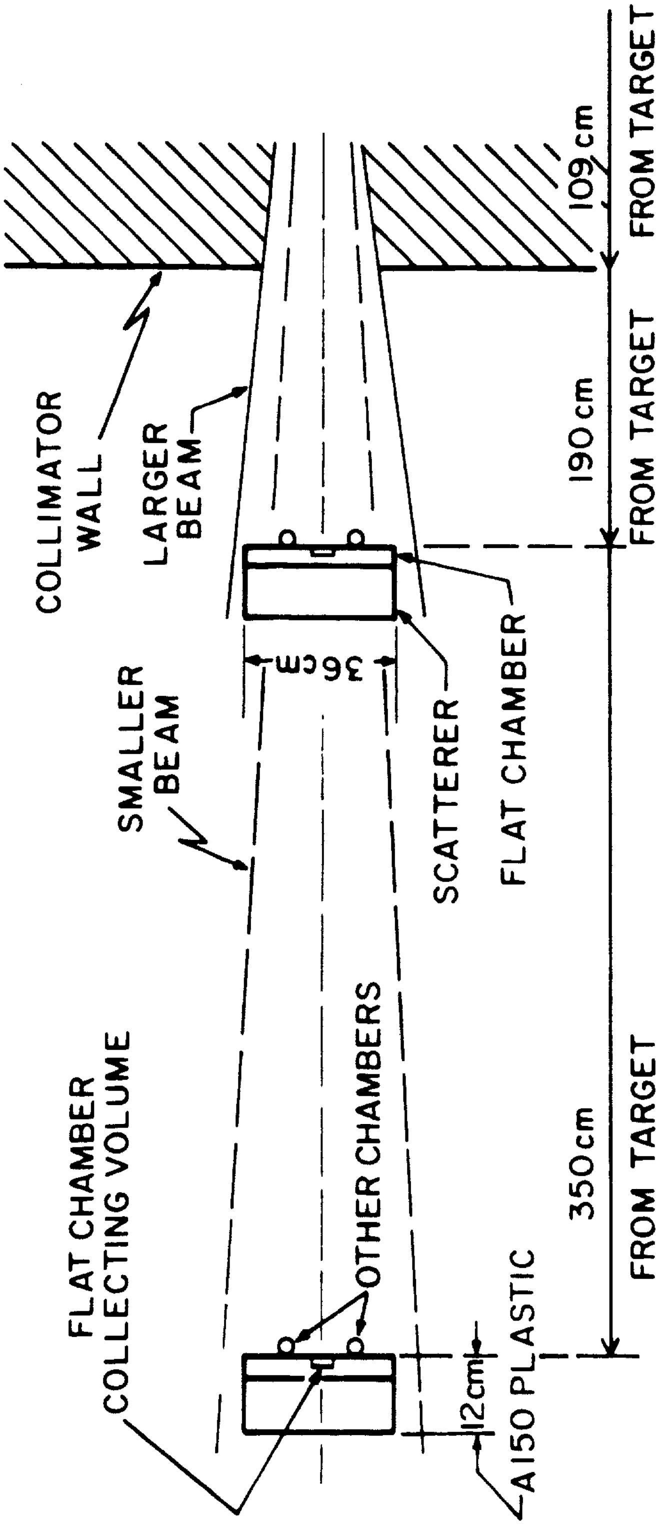

COLLIMATOR WALL
109 cm FROM TARGET
LARGER BEAM
190 cm FROM TARGET
36 cm
SCATTERER
FLAT CHAMBER
SMALLER BEAM
FLAT CHAMBER COLLECTING VOLUME
OTHER CHAMBERS
350 cm FROM TARGET
12 cm
A150 PLASTIC

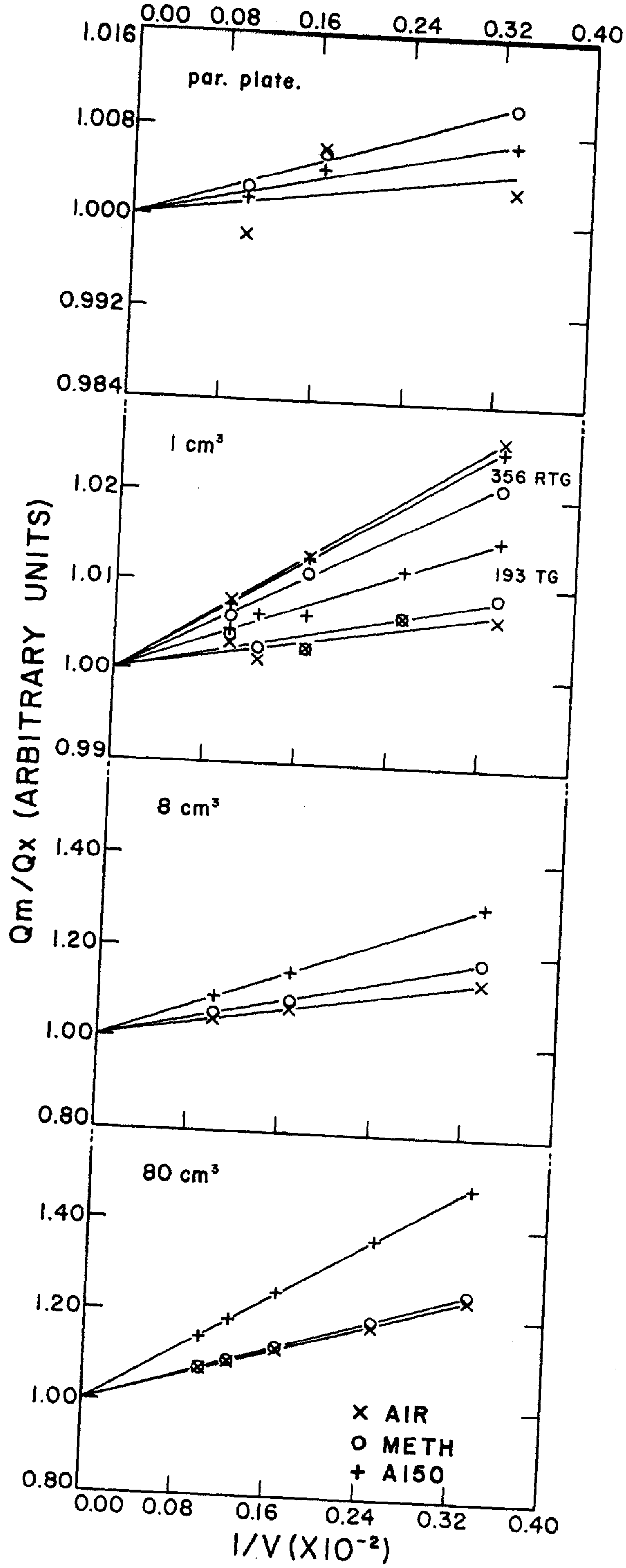
0.00 0.08 0.16 0.24 0.32 0.40
1.016
1.008
1.000
0.992
0.984
par. plate.
1 cm³
1.02
1.01
1.00
0.99
356 RTG
193 TG
8 cm³
1.40
1.20
1.00
0.80
80 cm³
1.40
1.20
1.00
0.80
Qm/Qx (ARBITRARY UNITS)
× AIR
O METH
+ A150
0.00 0.08 0.16 0.24 0.32 0.40
1/V (X10⁻²)

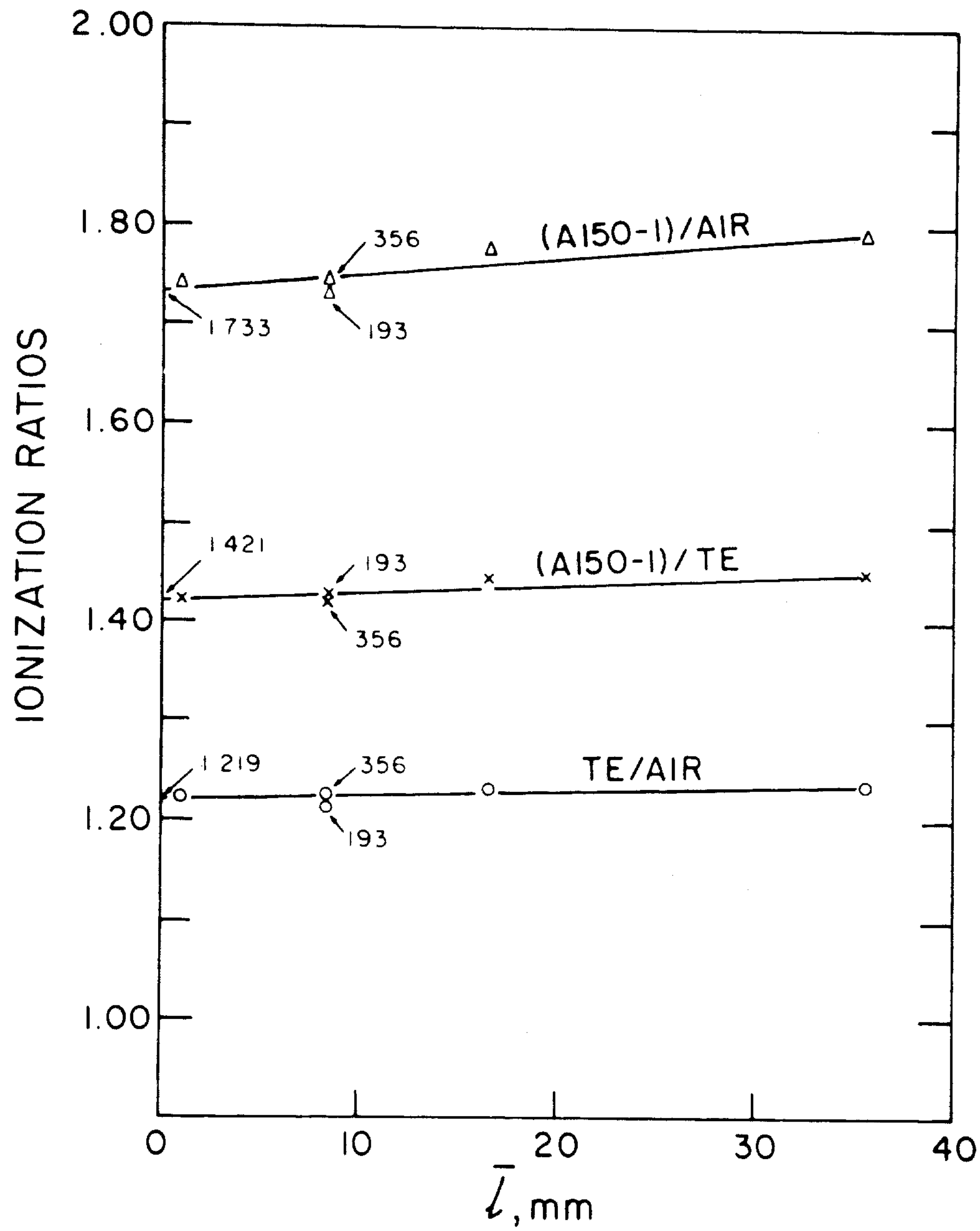
2.00
1.80
1.60
1.40
1.20
1.00
IONIZATION RATIOS
(A150-1)/AIR
356
1733
193
(A150-1)/TE
1421
193
356
TE/AIR
1219
356
193
0
10
20
30
40
$\bar{l}$, mm